Coupling COMIS airflow model with other transfer phenomena

E. A. Rodríguez

Energetical Engineering and Fluidmechanics Department ETSII, Seville University, Seville E-41012 (Spain)

F. Allard

Centre de Thermique INSA de Lyon, URA CNRS 1372, Bat 307, INSA, F-69621 Cédex, Villeurbanne (France)

Abstract

One of the main characteristics of thermal and fluid mechanical behaviour of buildings is that it is dominated by coupled heat and mass transfer phenomena. In this paper we describe the main phenomena influencing the behaviour of buildings and propose a general formulation of these coupled phenomena. We then apply this formalism to two important problems. The first one deals with the coupling between a multizone thermal model and a multizone airflow model. The second one presents the coupling between the transport of pollutants and airflow calculation in a multizone building. In order to illustrate our proposition we give various kinds of examples of coupled configuration.

1. Introduction

Improving performance and quality of buildings must be the first aim of any designer. Towards this end a large number of numerical models have been developed in recent decades. Most of these models were at first devoted to particular aspects of the problem. After the energy crisis, for example, a strong effort was made to predict the thermal behaviour of buildings and to limit their energy losses.

Strong assumptions were usually made in these models about transfer phenomena such as airflow distribution or transport of pollutants. Yet, significant improvements of the thermal quality of building envelopes were made in recent years. However, problems appeared before long as people became more sensitive to comfort and health in buildings, and the first generation of models are no longer sufficient.

Comfort is a generic word that might, in these circumstances, be defined as the state of a person who does not prefer any other environmental conditions to the actual ones. Although "comfort" has subjective components, varying in meaning with every occupant, "average comfort" can be related to environmental conditions [1]. These are quantified by a set of physical quantities which enables us to know whether or not a certain situation is within the comfort range. These variables are mainly air temperature, air humidity, temperature of surrounding surfaces, noise level, lighting level, thermal radiation level, air velocity, and concentrations of irritant and odorous pollutants.

Any attempt to predict these variables must, of necessity, pass through a theoretical modelling process using the physical laws governing their evolution. Unfortunately, aside from noise and lighting which can usually be treated independently, most of the variables cannot be considered separately.

In this paper we focus on the coupling processes between thermal and fluid mechanical problems. We describe a general formalization of these coupled phenomena and give two examples of couplings. The first deals with the coupling between COMIS airflow model and a multizone thermal model, and the second with the coupling between a pollutant transport model and COMIS.

2. General description of thermal and fluid mechanical couplings in buildings

2.1. General description of transfer phenomena in buildings

In general terms the detailed simulation of thermal and fluid mechanical behaviour of buildings calls for the definition of the transient behaviour of the

elements composing the building — with external and internal influences as boundary conditions.

The external influences are:
— solar radiation
— outdoor air temperature
— other external temperatures of sky, ground and surrounding surfaces
— wind conditions
— outdoor air humidity
— outdoor concentration of pollutants.

The more common internal inputs are heat gains derived from lighting, occupants and miscellaneous equipment, and humidity and pollutants.

A building can be described as a complex system made up of solid heterogeneous elements (either opaque or semi-transparent), liquid elements (water walls, solar ponds, water films, etc.) and gaseous elements (mainly polluted and humid air). Large numbers of heat and mass transfer mechanisms exist between these elements:

— external convection (usually forced) between the external surfaces and the outdoor air;
— internal convection (usually natural or mixed) between the internal surfaces of the envelope components, occupants, lighting fixtures, etc., and the indoor air;
— shortwave radiation coming from the sun and in some cases from the internal heat sources;
— external longwave radiation between envelope surfaces and the sky, surrounding buildings and ground;
— internal longwave radiation between internal surfaces, and between these and the internal gains;
— fluid flow through cracks and openings between the building and the outdoor, or between zones of the building.

Most of the detailed building simulation programs [2–7] have retained some basic and well-contrasted hypotheses in order to represent this complexity. These are mainly:

— one-dimensional conduction through walls (except ground-coupled structures and thermal bridges);
— grey and diffuse radiant behaviour of surfaces (shortwave and longwave);
— linearized longwave radiant exchange between interior surfaces;
— uniform room air temperatures.

In spite of these hypotheses the problem of simulating a building is still complex and all the heat and mass transfer modes are coupled. In a first classification we can easily identify three levels of coupling:

● conduction, convection and radiation heat transfers appearing together in each element of the building, and being coupled to each other by the temperature field;

● radiation heat transfer in any enclosure providing a second kind of coupling between all the internal surfaces;

● an interzonal coupling taking place via conduction (through walls separating two rooms), via radiation (through semi-transparent media between two spaces) and/or via airflow between rooms.

Differences between the existing detailed models [3–7] dealing with these coupling effects are found partly in the modelling techniques concerned with the transfer phenomena through the building elements and partly in the coupling definition and solving procedures. Nevertheless, thermal and fluid mechanical couplings can be described in a general formalism.

2.2. General formalism of thermal and fluid mechanical couplings in buildings

In order to describe the general coupling effects in a building simulation problem, it is useful to establish the modelling procedure for both thermal and fluid mechanical problems first. Any of the modelling techniques in the thermal problem can lead us to a set of equations coupling the indoor surface temperatures and the room air temperatures.

Each internal surface temperature is defined by the thermodynamic equilibrium of the surface submitted to conduction, convection and radiation heat transfers. This balance equation relates, nonlinearly, all the N internal surface temperatures of the building T_{SI}, and all the NZ room air temperatures T^J connected to the surface being considered:

$$F_{SI}(T_{S1},\ldots,T_{SI},\ldots,T_{SN},\ T^1,\ldots,T^J,T^{NZ})=0 \qquad (1)$$

Moreover, the thermal state of each zone of a building is represented by its convective equilibrium, so enabling us to define a representative air temperature as state variable. The writing of an enthalpy balance for the zone under consideration leads us to a first-order differential equation relating air temperature to the surface temperatures of this zone (convective effect of walls) and to all the other zone air temperatures (interzone air movement). The discretization of the derivatives in these balance equations gives a set of algebraic expressions:

$$F_J^T(T_{S1},\ldots,T_{SI},\ldots,T_{SN},T^1,\ldots,T^J,\ldots,T^{NZ})=0 \qquad (2)$$

The fluid mechanical modelling procedure used as a rule takes a very similar approach. Typically the dynamic state of each zone is represented by a reference pressure. Flow equations define the different links existing in the pressure network which defines the building's behaviour [3, 8]. The air-mass

balance in each zone constitutes then a nonlinear system of equations combining these pressures:

$$F_J^F(P^1,\ldots,P^J,\ldots,P^{NZ})=0 \qquad (3)$$

To be rigorous, eqn. (3) must include the air density of each node. These densities are functions of absolute pressure, temperature, humidity and concentration of any pollutant in the zone. Consequently, and in order to close the problem, it is necessary to formulate the balance of the additional species (water vapour and pollutants), for each zone.

In general form the water vapour balance of each zone relates all the zone-specific humidities (by the interzonal airflows) and the temperatures of surfaces and air zone (due to condensation/evaporation phenomena):

$$F_J^W(W^1,\ldots,W^J,\ldots,W^{NZ},T_{S1},\ldots,T_{SI},\ldots,T_{SN},T^1,$$
$$\ldots,T^J,\ldots,T^{NZ})=0 \qquad (4a)$$

In a general way we can write a similar equation for any pollutant k in zone j:

$$F_J^K(C_K^1,\ldots,C_K^J,\ldots,C_K^{NZ},T_{S1},\ldots,T_{SI},\ldots,T_{SN},T^1,$$
$$\ldots,T^J,\ldots,T^{NZ})=0 \qquad (4b)$$

where C_K^J is the concentration of pollutant K in zone J.

After the formalization of the different phenomena and the definition of state variables representing the behaviour of each controlled volume or zone, the closure of the complete problem must be checked.

State variables:
surface temperatures $(T_{SI}) \longrightarrow$ NS
zone air temperatures $(T^I) \longrightarrow$ NZ
zone reference pressures $(P^I) \longrightarrow$ NZ
zone specific humidities $(W^I) \longrightarrow$ NZ
zone concentration of pollutant $(C_k^I) \longrightarrow$ NZ

Balance equations:
thermodynamical surface equilibrium $\longrightarrow$ NS
zone enthalpy balance $\longrightarrow$ NZ
zone air mass balance $\longrightarrow$ NZ
zone water vapour balance $\longrightarrow$ NZ
zone pollutants balance $\longrightarrow$ NZ

These equations are not independent since the mass balance of air defining the pressures depends on all the other state variables. The other balance equations require the definition of the interzonal airflows resulting in the pressure network resolution.

In summary, we obtain a set of simultaneous and nonlinear equations which, once solved, will give us the complete field of state variables, temperatures (of zones and indoor surfaces), reference pressures, specific humidities and pollutants concentrations. Though this complex methodology has been for-

mulated in a similar way before [9], it is not usually solved in this form. Modellers usually look for simpler formulations and solving techniques and therefore have to make additional assumptions in order to render both formulation and resolution easier.

The most common simplifications are the decoupling of coupled phenomena (solving thermal and fluid mechanical problems separately by iterative procedures [4, 6]; linearizing systems (longwave radiant exchange between zone surfaces in the thermal problem [7]; or using the Jacobian system to solve the pressure network system in the fluid mechanical problem [8]). These simplifications are justified in most cases in that not all couplings existing in a building are equally strong. This allows us to solve the strongest couplings by using values of former iterations in the values of the weakest couplings' variables.

To describe more accurately these different coupling effects, we describe two general cases found in building physics. The first deals with the coupling of a multizone airflow model with a thermal one, the second concerns the coupling between a multizone airflow model and a pollutant transport model.

3. Coupling thermal-fluid mechanical problems in S3PAS

3.1. Fundamentals of S3PAS code

S3PAS [10, 11] is a thermal building simulation code on a hourly basis. This program has been used as a host structure to couple a COMIS airflow model with a multizone thermal model. It distinguishes the three levels of coupling in a building already mentioned and solves them in a hierarchical way from the weaker to the stronger [12].

S3PAS deals with the first coupling by defining the surface temperatures of each internal wall. This is done by resolving the heat transfer problem in the most appropriate way for each building element.

The heat transfer by conduction in each element enclosing a space is expressed in a common formula whatever the method used to model the heat transfer through the selected element. This equation is:

$$Q_{ci}(t)=B_1+B_2\,T_{si}(t) \qquad (5)$$

where
T_i = equilibrium air temperature in zone i
$Q_{ci}(t)$ = conduction heat flow from the internal surface of element i at time t
$T_{si}(t)$ = surface temperature of the internal element i at time t
B_1, B_2 = constants which depend on properties of element i in former time steps.

This formulation allows for the modelling of the second level of coupling based on the thermal equilibrium of the internal surfaces of a zone.

For surface si we have:

$$B_1 + B_2 T_{si}(t) = h(T_{si}(t) - T_i(t))$$
$$+ \sum_{j=1}^{j=N} K_{ij} T_{sj}(t) - \Phi_c(t) \qquad (6)$$

where

$h(T_{si}(t) - T_i(t))$ represents the convective flow density exchanged between the surface si and the zone temperature T_i,

$\sum_{j=1}^{j=N} K_{ij} T_{sj}(t)$ represents the net longwave radiation flow density at the surface si,

$\Phi_c(t)$ represents a shortwave radiation flow density absorbed by surface si.

The conjunction of the N surface equations forms the following system in matrix notation:

$$[K]\{T_s\} - T_i\{h_{cv}\} = \{B\} \qquad (7)$$

From this matrix equation, surface temperatures can be expressed as a function of the zone temperature:

$$\{T_s\} = [K]^{-1}\{B\} + [K]^{-1}\{h_{cv}\}T_i \qquad (8)$$

In order to close the problem it is necessary to express the effect of the enclosing surfaces of a zone on the air enthalpy balance of that zone.

The first element of this balance is given by the total convective heat flux exchanged along all the surfaces of the enclosure. This flux named $Q_{cv})_{walls}$ is defined as follows:

$$Q_{cv})_{walls} = \sum_{k=1}^{k=N} h_{cvk} S_k (T_{sk} - T_i) \qquad (9)$$

in matrix form:

$$Q_{cv})_{walls} = \{h_{cv}S\}\{T_s\} - \left(\sum_{k=1}^{k=N} h_{cvk} S_k \right)\{T_i\} \qquad (10)$$

and by substituting the expression of $\{T_s\}$ given by eqn. (8) we obtain:

$$Q_{cv})_{walls} = PIND + COEFF.T_i \qquad (11)$$

where

$$PIND = h_{cv}[K]^{-1}\{B\}$$

$$COEFF = - \sum_{k=1}^{k=NS} h_{cvk}.S_k + \{h_{cv}S\}[K]^{-1}\{h_{cv}\}$$

The interzonal conductive and radiant couplings are implicitly included in the vector $\{B\}$ of the enclosure equations. They have been included in

that way because their coupling effect is much weaker than the effect of interzonal air movement.

Finally, the strongest coupling between zones is due to the multizone airflows resolving the air balances together with the airflow problem. These balances are expressed by means of the following differential equations written for each zone or controlled volume, defined in the building description.

$$V_I C_{pI} \frac{d\rho_I T_I}{dt} = Q_{cv})_{walls} + Q_{cv})_{gains}$$
$$+ \sum_{J=0}^{J=NZ} m'_{JI} C_{pJ} T_J - \sum_{J=0}^{J=NZ} m'_{IJ} C_{pI} T_I \qquad (12)$$

where

V_I = control volume of zone i

C_{pI} = specific heat of air in zone i

$Q_{cv})_{walls}$ = convective heat flow from all the internal surfaces of zone i

$Q_{cv})_{gains}$ = convective heat flows from internal sources or sinks in zone i

m'_{IJ} = air mass flow rate from zone i to zone j

T_I = convective equilibrium air temperature in zone i.

The main hypotheses assumed in eqn. (12) are:
— uniform temperature in each zone;
— time-derivative of the specific heat of air in each zone is neglected;
— no thermal effect of other pollutants.

According to the dynamic treatment the mass-air balance in each zone is expressed in an unsteady state:

$$V_I \frac{d\rho_I}{dt} = \sum_{J=0}^{J=NZ} m'_{JI} - \sum_{J=0}^{J=NZ} m'_{IJ} \qquad (13)$$

The left side of eqn. (12) is then written as follows:

$$V_I C_{pI} \frac{d\rho_I T_I}{dt} = V_I C_{pI} \rho_I \frac{dT_I}{dt} + V_I C_{pI} T_I \frac{d\rho_I}{dt} \qquad (14)$$

By substituting eqn. (14) in eqn. (12) and using the mass balance equation, eqn. (13), we obtain:

$$\rho_I V_I C_{pI} \frac{dT_I}{dt} = Q_{cv})_{walls} + Q_{cv})_{gains}$$
$$+ \sum_{J=0}^{J=NZ} m'_{JI} (C_{pJ} T_J - C_{pI} T_I) \qquad (15)$$

The conjunction of eqn. (15) applied to all the zones forms a system of first-order differential equations with the air temperatures of each zone as unknowns.

In relation to its internal structure, S3PAS is a modular code with a steering controller and different modules. These modules either simulate the thermal behaviour of certain elements of the building or

solve the different couplings between them. Other modules do not correspond exactly with real elements and simply calculate aspects such as solar position, shading effect and boundary conditions.

The various modules are the following:

• Meteorological: calculates the solar position and the direct normal radiation;

• Shadows I: determines the solar obstruction of remote obstacles;

• Shadows II: determines the effect on the solar gains through each building opening due to shading devices;

• TSA: calculates the total external boundary condition of an element in terms of the sol-air temperature;

• Envelope Wall: simulates the thermal behaviour of an opaque multilayer wall of the exterior envelope of the building;

• Interzone Wall: simulates the thermal behaviour of an opaque multilayer wall connecting two simulated zones of the building;

• Envelope Glazing: simulates the behaviour of an envelope formed by semi-transparent walls;

• Interzone Glazing: simulates a semi-transparent wall that connects two simulated zones;

• Floor: simulates ground-coupled structures;

• Trombe Wall: simulates a Trombe wall;

• Collect- Rock Bed: simulates the system formed by an air solar collector and a rock-bed storage system;

• Zone: supports the coupling between the different elements of a zone;

• Building: couples all the simulated zones of the building by calculating the airflows and delivering the thermal balances.

At each time step the steering program calls the different modules in the following order:

— the modules related to boundary conditions (Meteorological, Shadows I and II and TSA);

— the simulation of the building itself begins in the element modules which send a pair of values (B1 and B2) to the next module (zone);

— a module "Zone" for each zone to perform the longwave radiant coupling between the surfaces of each zone and a new pair of values (PIND and COEFF) is sent to next module (Building);

— the module "Building" to couple all the zones in terms of airflows and air thermal balances.

3.3. Coupling problems and strategies

The main problem found in the resolution of the system of differential equations represented by eqn. (15) is the need for discretization of the time-derivatives of zone temperatures. Those derivatives are usually replaced by backward differences of the temperatures divided by the time step:

$$\frac{dT_i}{dt} \# \frac{T^k{}_i - T^{k-1}{}_i}{\Delta t} \tag{16}$$

The discretization of eqn. (15) gives

$$\rho_i V_i C_{pi} \frac{T^k{}_i - T^{k-1}{}_i}{\Delta t}$$

$$= \text{PIND}_i + \text{COEFF}_i T^k{}_i + Q_{cv})_{\text{gains}}$$

$$+ \sum_{j=0}^{j=NZ} m'_{ji}(C_{pj} T^k{}_j - C_{pi} T^k{}_i) \tag{17}$$

The key question is which Δt should be chosen. One might think that the only requirement for Δt is accuracy of the derivative (the discretization error is proportional to Δt). However the error in the zone temperature may be lower due to a small value of the discretized derivative. In addition, the solving process is an iterative procedure between the airflow model (which calculates m'_{ij}) and the thermal model until zone temperatures converge. We should therefore be careful in choosing a time step so as to reach an acceptably accurate solution in as few iterations as possible.

The following method is used to set the time step.

(1) with an initial vector $\{T^{k-1}\}$ the airflow model calculates the matrix $[m'_{ij}]$.

(2) for each zone an effective ventilation temperature (EVT) is calculated as follows:

$$\text{EVT}_i = \frac{\displaystyle\sum_{j=0}^{j=NZ} m'_{ji}(C_{pj} T^k{}_j - C_{pi}) T^k{}_i}{\displaystyle\sum_{j=0}^{j=NZ} m'_{ji} C_{pi}} + T^{k-1}{}_i \tag{18}$$

and this temperature is an index of the average effect of multizone airflows on the zone temperature.

(3) the user can establish the maximum increase (or decrease) allowed in the zone temperature for each zone. Some examples are:
in terms of the calculated EVT:

$$T^k{}_j - T^{k-1}{}_i \leqslant \frac{\text{EVT}_i - T^k{}_i}{10} \tag{19}$$

or user defined:

$$T^k{}_j - T^{k-1}{}_i \leqslant \Delta T_{\text{max}} \tag{20}$$

(4) Once that increase or decrease is set, applying eqn. (16) to each zone (with T^{k-1} instead of T^k on the right side), we obtain a time step for each one and choose the minimum.

(5) The system of equations formed by all eqns. (16) is solved, obtaining the vector $\{T^k\}$.

(6) Successive iterations between airflow model and thermal balance can be performed until zone temperatures converge, but few iterations are likely to be needed after an optimized time step has been used.

(7) Return to stage 2 until the sum of former time steps is one hour.

This procedure is repeated on each time. It is worth noting that the formulation given by S3PAS to deal with the convective effect of walls on the zone air temperature is very flexible to be coupled in the zone balances, because it avoids further iterations over the conductive model.

The development of the complete set of equations describing the thermal and fluid mechanical behaviour of a building shows how strong are the couplings between these two transfer phenomena. However, in other cases, one transfer phenomenon is dominant and the coupling becomes weaker. To illustrate this point we present now the coupling of a pollutant transport model with an airflow model.

4. Coupling COMIS with a multizone pollutant transport model

As described in Section 2 the transport of concentrations in a multizone building leads to the definition of mass balance equations for each pollutant considered, in each controlled volume and at each time step of the period studied. These mass balance equations can be defined in a general manner as described by eqns. (4a) and (4b).

Even if the airflow model appears clearly as the leading phenomenon in most of the cases, the influence of high pollutant concentrations can change significantly the stack effect; it is no more possible then to consider each phenomenon separately and coupled analysis is necessary [13, 14] to describe accurately the combined effects of the various transport processes.

In this part we focus only on the coupling processes between airflow model and pollutant transport, and we describe a general formalization of these coupled phenomena.

4.1. Fundamentals of COMIS pollutant model

In parallel with the development of the multizone airflow model, we developed in COMIS a multizone transport model defining basically the mass balance of each pollutant in each zone of a building.

The mass variation in time of a specific concentration of a pollutant p in zone i is due to the divergence of pollutant mass flows through the boundaries of this control volume increased by internal sources. The main assumption here is that the concentration is well mixed in a zone and is transported from zone to zone by the flow of air. As far as we assume the concentrations being transported by the airflows, the first level of coupling between the two phenomena is given directly by the mass balance equation of each pollutant. Equation (21) describes this mass balance.

$$\frac{d(\rho_{ai}V_iC_{ip})}{dt} = \sum_{j=0}^{j=NZ}\sum_{k=1}^{k=NZ}m'a_{jik}(t)(1-\eta_{ji})C_{jp}(t)$$
$$- \sum_{j=0}^{j=NZ}\sum_{k=1}^{k=NZ}(m'a_{ijk}(t)+k_{ip})C_{ip}(t)+S_{ip}(t) \qquad (21)$$

where

V_i = volume of zone i

ρ_{ai} = density of dry air in zone i

C_{ip} = specific concentration of pollutant p in zone i

$m'a_{ijk}$ = mass flow of dry air between zones i and j through link k

$m'a_{jik}$ = mass flow of dry air between zones j and i through link k

η_{jik} = filter efficiency between zone j and i through link k

k_{ip} = reactivity of pollutant p in zone i

$S_{ip}(t)$ = source or sink term of pollutant p in zone i

$j=0$ outside conditions

NZ = number of zones

NK = number of links between two zones.

In eqn. (21), η_{jik} represents the filter effect of link k, between zones j and i on the incoming concentration. This effect affects the transported concentration and can represent a solid absorption along the path or any kind of reaction (chemical reaction, phase change, etc.) due to the contact of the pollutant with a solid material when flowing from one zone to the other.

k_{ip} that we call reactivity, is a general term to take into account chemical reaction, adsorption or desorption effect in solid materials, phase change or nuclear reactivity of a radioactive pollutant in the considered zone itself.

η_{jik} and k_{ip} can be defined either as constant values or as functions of other state variables than the concentrations. $S_{ip}(t)$ represents a source of indoor pollutant p in zone i.

One of the main problems in predicting the pollutant dispersion in a multizone building is the definition of the indoor or outdoor sources and the two terms we call reactivity and filter effect. Good compilation of data has been made by Traynor et al. [15, 16] and Tichenor et al. [17], but much more is needed in this field to reach a precise

characterization of the main indoor and outdoor sources.

The first term of eqn. (21) can be developed in

$$\frac{d(\rho_{ai}V_iC_{ip})}{dt} = C_{ip}\frac{d(\rho_{ai}V_i)}{dt} + \rho_{ai}V_i\frac{dC_{ip}}{dt} \qquad (22)$$

However in eqn. (22), $\frac{d(\rho_{ai}V_i)}{dt}$ is just defining the mass balance of dry air in zone i. This mass balance is also written as eqn. (23)

$$\frac{d(\rho_{ai}V_i)}{dt} = \sum_{j=0}^{j=NZ}\sum_{k=1}^{k=NK}m'a_{jik}(t) - \sum_{j=0}^{j=NZ}\sum_{k=1}^{k=NK}m'a_{ijk}(t) \qquad (23)$$

If we introduce the definition given by eqn. (23) in eqn. (21), we obtain a general definition of the concentration of pollutant p in zone i involving only the incoming flows.

$$\rho_{ai}V_i\frac{dC_{ip}}{dt} = \sum_{j=0}^{j=NZ}\sum_{k=1}^{k=NK}m'a_{jik}(t)(1-\eta_{ji})C_{jp}(t)$$
$$- \sum_{j=0}^{j=NZ}\sum_{k=1}^{k=NK}(m'a_{jik}(t)+k_{ip})C_{ip}(t)+S_{ip}(t) \qquad (24)$$

To integrate eqn. (24) in time, we use a purely implicit finite difference scheme. This method leads to the definition of a linear system of equations defining the field of concentrations at each time step. Under matrix notation we obtain:

$$[A]\{C_p^{t+\Delta t}\} = \{B\} \qquad (25)$$

with

$$A(i,j) = \sum_{k=1}^{k=NK}-m'a_{jik}^{t+\Delta t}(1-\eta_{jik}) \qquad i\neq j$$

$$A(i,i) = \frac{\rho_{ai}^tV_i}{\Delta t} + \sum_{j=0}^{NK}\sum_{k=1}^{k=NK}m'a_{jik}^{t+\Delta t}+k_{ip}^{t+\Delta t}$$

$$B(i) = \frac{\rho_{ai}^tV_i}{\Delta t}C_{ip}^t+S_{ip}^{t+\Delta t}$$
$$+ \sum_{k=1}^{k=NK}m'a_{0ik}^{t+\Delta t}(1-\eta_{0ik})C_{0p}^{t+\Delta t}$$

In the source term $B(i)$, the subscript 0 represents outside characteristics, these terms are introduced here as boundary conditions of the pollutant transport model at each time step.

In some cases like humidity transport, the variation of concentration may modify the density of air in various zones, influence the stack effect, and then may change significantly the multizone mass flow distribution.

We so define the second level of the coupling process between the two transfer phenomena by taking into account the effect of concentration on the definition of the density field which is one of the driving forces for the airflow distribution.

The air density of moist air with NP pollutants is given by eqn. (26).

$$\rho = P\left(1+XH+\sum_{i=1}^{i=NP}C_i\right)\bigg/\bigg[287.055(T+273.15)$$
$$\times\left(1+XH\cdot\frac{28.9645}{18.01534}+\sum_{i=1}^{i=NP}C_i\cdot\frac{28.9645}{MM_i}\right)\bigg] \qquad (26)$$

As pointed out in the preceding Section, an important problem when coupling different transfer phenomena is the definition of a reasonable choice for the time step of the simulation.

4.2. Selection of the time step

As a first approximation, we assume that the leading phenomenon in eqn. (24) is the transport of concentrations by the interzonal airflows. We neglect the filter effects, the reactivity and the presence of sources in order to get a rough estimate of the concentration in zone i. With all these assumptions, eqn. (24) has an analytical solution and a good estimate of the concentration of pollutant p in zone i is given by an exponential law

$$C_{ip} = A\exp\left[\left(\frac{\sum_{j=0}^{j=NZ}m'a_{ji}}{-\rho_{ai}V_i}\right)t\right] \qquad (27)$$

where $m'a_{ji}$ represents the total dry airflow coming from zone j to zone i and A is a constant defined by the boundary conditions of the problem.

The time constant of this particular problem is then given by

$$\tau_i = \frac{V_i\rho_{ai}}{\sum_{j=0}^{j=NZ}m'a_{ji}} \qquad (28)$$

As first approximation, the condition to fulfill for the time step can then be taken as:

$$\Delta t \ll \min_{i=1}^{i=NZ}\tau_i \qquad (29)$$

5. Illustrative examples

In this Section we present two kinds of examples related to the coupling of thermal and airflow models, and pollutant transport and airflow distribution.

5.1. Coupled effect of airflow distribution and thermal behaviour of a single cell

Figure 1 shows a single-zoned cell. North and south facades are exposed to outdoor temperature and each has a large opening. The other walls are connected to a controlled environment at 20 °C.

5.1.1. Influence of the thermal characteristics of the walls

Different types of wall composition are considered:
(1) adiabatic walls;
(2) multilayered heavy wall (see description in Table 1);
(3) conductive walls.

The curves in Fig. 2 are plotted to show the evolution of indoor temperature for the three types of cell construction. We can observe how close to the outdoor temperature is the indoor one in the adiabatic cell. This is due to the major role of the air movement compared with the meaningless wall conductive heat flow. As the wall construction becomes more conductive, the indoor temperature swing is more influenced by the constant boundary condition of 20 °C by means of the conductive flow through the walls.

This simple example shows the great differences existing in the global behaviour of the cells when dealing with different wall properties in an apparently airflow-driven case.
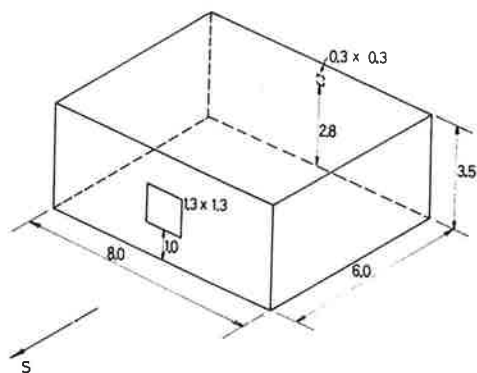
5.1.2. Influence of the permeability characteristics of the cell

In this example we fix the wall construction of the cell (the multilayered heavy wall of case 2) and distinguish three cases by changing the size and position of the large openings in north and south facades to make the cell successively more airflow-driven. Figure 3 shows these facades for the three cases tested.

The indoor temperature swings of the three cells exposed to the same meteorological conditions as in Example 1 are represented in Fig. 4. The main conclusion of this example is that despite being a case which is strongly driven by the airflow phenomenon, the conductive effect of the envelope is always relevant and avoids the indoor temperature becoming equal to the outdoor conditions.

5.1.3. Selection of the time step

In this example the effect of calculating an optimized time step in the temperature evolution of a test case is checked. The choice of an optimized time step for the airflow problem is related to the relative effect of air movement in indoor test cell conditions.

This is an unreal case because all the cell walls are exposed externally to a fixed-temperature environment of 10 °C. Initially the indoor temperature is kept at 20 °C. At $t = 0$ the window is instantly opened and the indoor temperature of the cell is allowed to vary freely. After a certain period of time the cell reaches a steady state in which both indoor air and walls are cooled to 10 °C.

Initially there exists a gradient of 10 °C between indoor and outdoor so the air movement is very efficient through the large opening. This fact provokes a rapid change in the air temperature of the cell. Figure 5 shows the difference obtained between choosing $\Delta t = 3600$ s and an optimized time step in the simulation of this case.

The maximum gap appears in the first time step (only three-tenths of a degree Celsius) and the model with $\Delta t = 3600$ s presents a faster response. There

Fig. 1. Geometrical definition of the single cell.

TABLE 1. Description of the multilayered walls

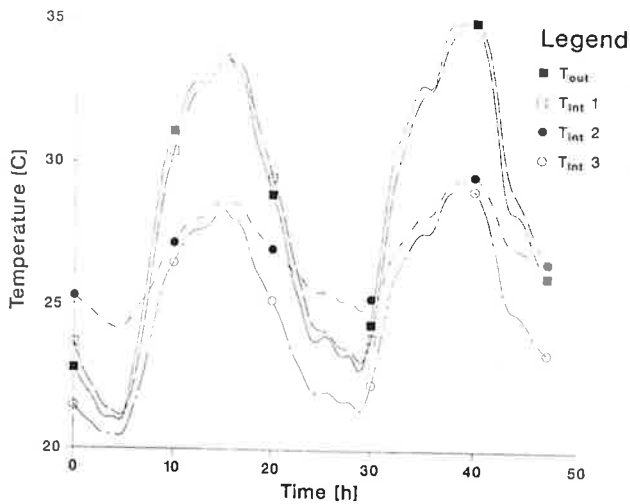| Layer	Thickness	Thermal conductivity	Density	Specific heat	Thermal resistance
Brickwork	0.10	0.84	1700	800	–
Air layer	0.05	–	–	–	0.18
Foam insulation	0.05	0.04	10	1400	–
Concrete block	0.10	0.51	1400	1000	–
Plaster	0.02	0.26	800	1000	–

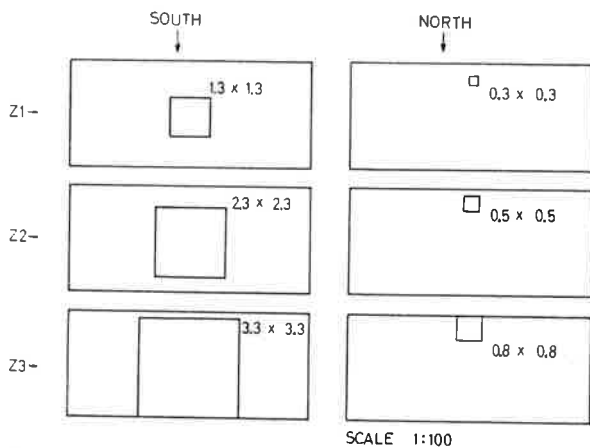Fig. 2. Evolution of the indoor temperatures of the three cells.

Fig. 3. Geometrical definition of tested facades.

is no difference in the time in which steady state is reached.

5.2. Coupled effect between a multizone airflow model and a pollutant transport one

5.2.1. Weak coupling configuration

In the following example, we consider a simple configuration with two rooms as described in Fig. 6. Room 1 has a volume of 468 m³ and room 2 is 54 m³. The initial concentrations in both rooms are 1000×10^{-6} g/kg dry air, and the outside concentration is 100×10^{-6} g/kg dry air. The mass flow rates described on Fig. 6 correspond to a configuration of one air change per hour.

Figure 7 shows the evolution of the indoor concentration in both rooms during one hour when varying the air exchange rate. As the concentrations are directly transported by the airflow, the results obtained show a direct dependency of the concentration level with the air change rate. In this first

example, the effects of concentration on the density field are too small to perturb the flow distribution.

5.2.2. Complete coupling configuration

In order to illustrate the coupling between concentration transport and airflow distribution, we consider the effect of humidity content on the airflow through a large opening separating two zones. The doorway is 2.0 m high and 0.8 m wide and its discharge coefficient is set to 0.65. At first we consider a temperature difference varying between the two rooms. In the second case the two zones are isothermal (20 °C), and we vary only the water vapour content on one side of the opening. Figure 8 shows the results obtained in comparing these two configurations. A strong driving effect of the humidity content appears here. At 20 °C air may contain up to 15 grams of water vapour per kilo of dry air, we show here that a difference of concentration of 5 g/kg dry air has roughly the same effect as a 1 °C difference.

6. Conclusions

In this paper we described in a general way the main coupling effects found in building physics when dealing with thermal behaviour, airflow distribution or pollutant transport. We define at first a general formalism to describe in a global way all these coupled heat and mass transfer phenomena and we developed two configurations frequently found in buildings.

The first corresponds to the coupling of a thermal model and a multizone airflow one. In this case, the coupling between the heat and mass transfer phenomena appears very clearly and is very strong. The temperature field modifying the density distribution is one of the important phenomena driving the airflows and the airflow distribution is one of the most important effects defining the enthalpy balance of a zone. In this case these two transfer phenomena can no longer be solved separately.

In the second case, when coupling a pollutant model with an airflow model, one may think that the coupling due to the density variation is too weak and can be neglected. In fact there are many situations in buildings where this assumption is wrong when dealing with important concentrations.

The examples we present are only illustrative, and much more work is needed to see the sensibility of models to the assumptions taken into account in the coupling modelling. However, they enable us to show the absolute necessity of coupled solutions.
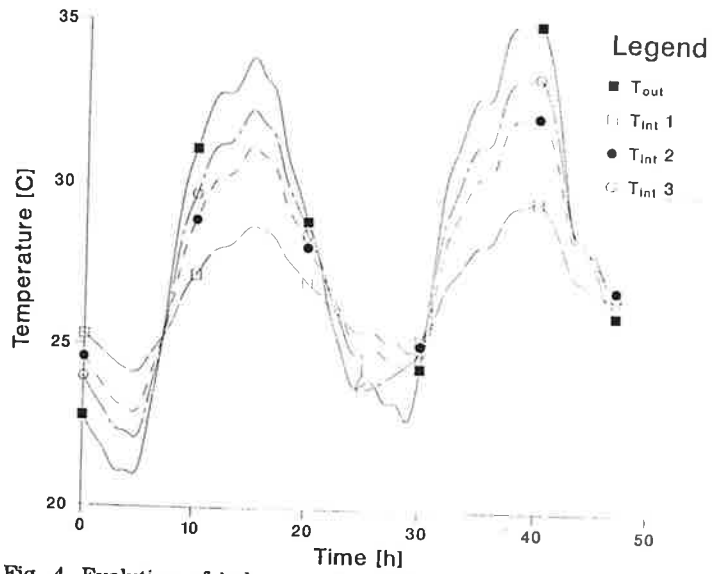
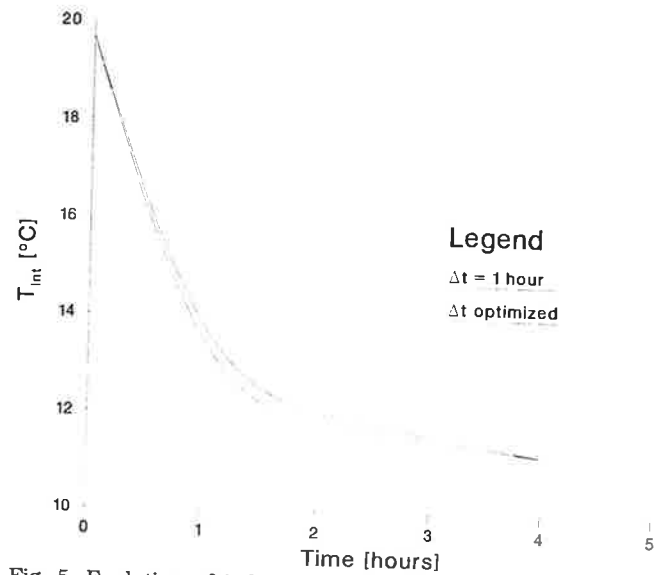Fig. 4. Evolution of indoor air temperatures.

Legend
- T_{out}
- T_{int} 1
- T_{int} 2
- T_{int} 3

Fig. 5. Evolution of indoor air temperatures with time.

Legend
Δt = 1 hour
Δt optimized

$V_1 = 468 \ m^3$

$V_2 = 54 \ m^3$

0.10 kg/s

0.045 kg/s

0.03 kg/s

0.13 kg/s

0.015 kg/s
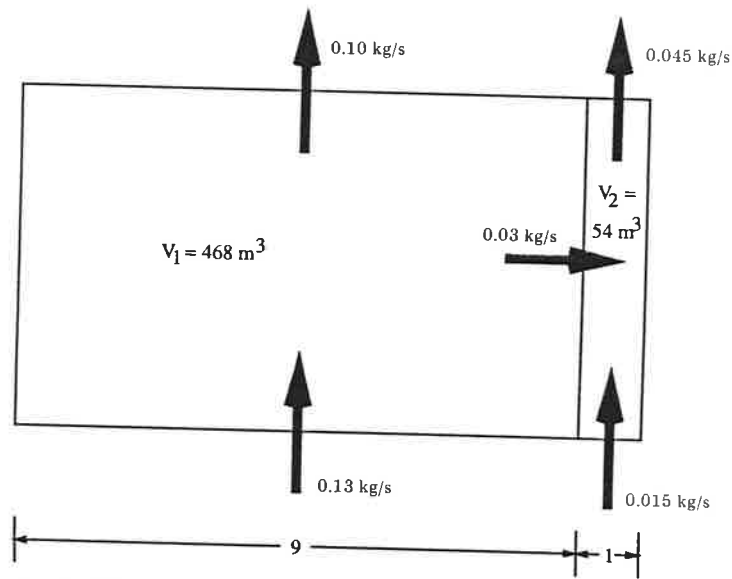
Fig. 6. Schematic description of the test case.

K = 0.0 kg/s

K = 0.1 kg/s

K = 0.25 kg/s
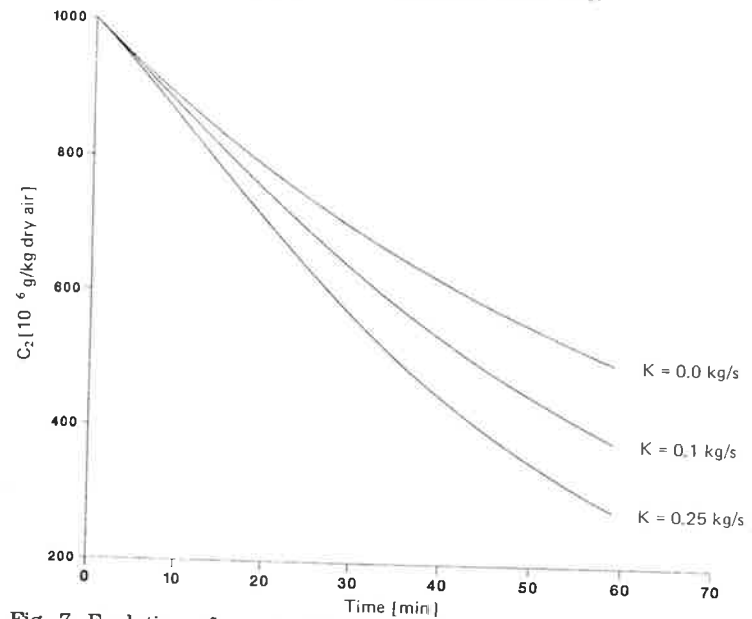
Fig. 7. Evolution of concentration in both rooms with various air change rates.
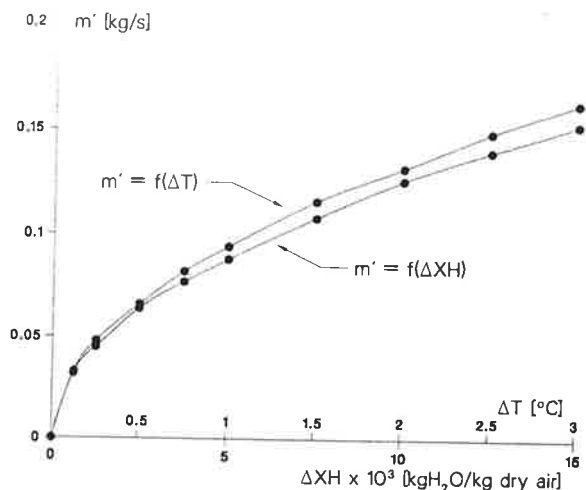
Fig. 8. Influence of water content difference between two rooms on the exchanged airflow.

η filter efficiency $(0 \leqslant \eta \leqslant 1)$
constant of dry air $= 287.055$ J/kg.K
molar mass of air $= 28.9645$ g
molar mass of water vapour $= 18.0153$ g

Nomenclature

B_1, B_2	constants
C	specific concentration (kg/kg dry air)
C_p	Specific heat of air (J/kgK)
F	functional form
h	convection exchange coefficient (W/m²K)
K	radiation exchange function
k	reactivity (kg/s)
MM	molar mass (g)
m'_{IJ}	air mass flow rate from zone i to zone j (kg/s)
$m'a_{ijk}$	mass flow of dry air between zones i and j through link k (kg/s)
N	number of internal surfaces
NK	number of links between two zones
NP	number of pollutants in the mixture
NZ	number of zones
P	reference pressure (Pa)
Q_c	conduction heat flow (W)
Q_{cv}	convective heat flow (W)
S	source or sink term of pollutant in a zone (kg/s)
T	air temperature (°C)
T_s	surface temperature (°C)
V	volume (m³)
XH	specific humidity (kg water/kg dry air)
ρ	density of air (kg/m³)
ρ_a	density of dry air (kg/m³)

References

1 P. O. Fanger, *Thermal Comfort*, McGraw-Hill, New York, 1973.
2 *DOE-2.1 Reference Manual*, Lawrence Berkeley Laboratory, 1981.
3 G. N. Walton, Air flow and multiroom thermal analysis, *ASHRAE Trans.*, 88 (Part 2) (1982).
4 A. Roldan, Etude Thermique et Aeraulique des Enveloppes de Batiment — Influence des Couplages Interieurs et du Multizonage (Thermal and airflow study of buildings envelopes. Influence of thermal couplings and multizoning effects), *Ph.D. Thesis*, I.N.S.A., Lyon, 1985.
5 S. Alvarez, Analysis Dinamico del Comportamiento Termico de Edificios (Transient analysis of thermal behavior of buildings), *Ph.D. Thesis*, E.S.I.I., Seville, 1986.
6 J. Clarke and D. McLean, *ESP, A Building and Plant Energy Simulation System, Version 6, Release 8. ABACUS*, University of Strathclyde, Glasgow, 1988.
7 *S3PAS 1.0, Simulacion de Sistemas Solares Pasivos — Manual de Usuario* (S3PAS 1.0, Solar passive system modeling — User guide) E.S.I.I., Seville, 1986.
8 G. N. Walton, A computer algorithm for predicting infiltration and interroom airflows, *ASHRAE Trans.*, 90 (Part 1) (1984).
9 J. Axley, The coupled airflow and thermal analysis problem in building airflow system simulation, *ASHRAE Trans.*, 95 (Part 2) (1989).
10 *Metodo de Simulacion y Calculo de Sistemas Pasivos en Relacion con su Comportamiento Termico, Informe de Avance n:1*, Catedra de Termotecnia, E.S.I.I., Seville, 1986.
11 *Metodo de Simulacion y Calculo de Sistemas Pasivos en Relacion con su Comportamiento Termico, Informe de Avance n:2*, Catedra de Termotecnia, E.S.I.I., Seville, 1987.
12 E. A. Rodriguez, *Acoplamientos Termicos en Edificios* (Thermal couplings in buildings), E.S.I.I. Report, Thermal Energy and Fluid Mechanics Department, E.S.I.I., Seville, 1988.
13 R. Grot and J. Axley, The development of models for prediction of indoor air quality in buildings, *Proc. 8th AIVC Conf., Uberlingen, FRG, 1987*.
14 J. Axley, Multi-zone dispersal analysis by element assembly, *Build. Environ.*, 24 (1989) 113–130.
15 G. W. Traynor et al., *Macromodel for Assessing Residential Concentrations of Combustion-generated Pollutants: Model Development and Preliminary Predictions for CO, NO₂ and Respirable Suspended Particles*, Report LBL-25211, Lawrence Berkeley Laboratory, Berkeley, CA, Jan. 1989.
16 G. W. Traynor et al., The effects of infiltration and insulation on the source strengths and indoor air pollution from combustion space heating appliances, *APCA J.*, 38 (1988) 1011–1015.
17 B. A. Tichenor, L. E. Sparks, J. B. White and M. D. Jackson, Evaluating sources of indoor air pollution, *Proc. 81st Annual Meet. APCA, Dallas, TX, June 19–24, 1988*.